Adaptive Proxy-based Robust Control Integrated with Nonlinear Disturbance Observer for Pneumatic Muscle Actuators

Yu Cao, *Student Member, IEEE,* Jian Huang, *Senior Member, IEEE,* Caihua Xiong, *Member, IEEE,* Dongrui Wu, *Senior Member, IEEE,* Mengshi Zhang, *Student Member, IEEE,* Zhijun Li, *Senior Member, IEEE,* Yasuhisa Hasegawa, *Member, IEEE*

***Abstract*—In Pneumatic Muscle Actuators (PMAs)-driven robotic applications, there might exist unpredictable shocks which lead to the sudden change of desired trajectories and large tracking errors. This is dangerous for physical systems. In this paper, we propose a novel adaptive proxy-based robust controller (APRC) for PMAs, which is effective in realizing a damped response and regulating the behaviors of the PMA via a virtual proxy. Moreover, the integration of the APRC and the nonlinear disturbance observer (NDO) further handles the system uncertainties/disturbances and improves the system robustness. According to the Lyapunov theorem, the tracking states of the closed-loop PMA control system are proven to be globally uniformly ultimately bounded through two motion phases. Extensive experiments are conducted to verify the superior performance of our approach, in multiple tracking scenarios.**

***Index Terms*—Pneumatic muscle actuator, adaptive proxy-based robust control, two-phase stability analysis.**

I. INTRODUCTION

DUE to the attractive characteristics, i.e., high power/weight ratio, no mechanical parts, low cost, etc [1], the Pneumatic Muscle Actuator (PMA) has been widely used in a variety of fields, especially exoskeletons that are effective in power augmentation and rehabilitation training [2]–[4]. Its driving force is converted from the air pressure of the inner bladder, which has the features of nonlinearity, hysteresis, and time-varying parameters [5], making its modeling and control very challenging. Different control strategies have been proposed for the PMA, including PID-based control [6], nonlinear model predictive control [7], [8], sliding mode control (SMC) [9], fuzzy control [10], adaptive control [11], dynamic surface control [12], etc. Unfortunately, an accurate mathematic model of the PMA is very difficult to obtain in practice which causes difficulties in precise control. Meanwhile, the traditional PID control, a typical model-free strategy, works in the position control of the PMA. However, some significant issues should be taken into account. First, the high-gain PID controller may cause oscillation and can hardly realize satisfactory performance in the physical PMA applications, due to the slow response of the PMA and limited sampling rate, etc. Second, the PMA is widely used in the field of robot actuation and industry, in which the load, running amplitude and frequency may change within a certain task. The traditional PID controller with a set of fixed control parameters may not meet the requirements of these applications. Next, from a theoretical viewpoint, it is difficult to theoretically prove the stability of the closed-loop system when no theoretical model is involved. Thus, there is still a strong demand for robust PMA control.

In robotic applications, the idea of using a proxy is common because a proxy enables robots to track the reference with a damped response to unexpected impacts, which results in the improvement of the system security and performance [13]. Whereas the physical proxy requires a light-weight and compact mechanism that leads to difficulties for designation. The virtual proxy is a remedy to fulfill the requirement of robot control. A typical strategy called proxy-based sliding mode control (PSMC) [14], which assumes that a zero-quality virtual proxy exists between the controlled object and the desired trajectory, is significantly a model-free strategy. Damme [15] presented a PSMC for a two-degree-of-freedom planar manipulator actuated by Pleated Pneumatic Artificial Muscles, and such a strategy of position control was developed for piezoelectric-actuated nanopositioning stages in [16]. Another approach supposed that there was a free space around the proxy for the impedance control of a cable-driven system [17]. However, most proxy-based strategies lack stability analysis or depend on a strong conjecture (e.g., see Conjecture 1 in [14]). Therefore, this kind of strategies demands further investigation to establish a sound theoretical foundation.

The robustness of the control strategy is another significant issue for robotic systems. Although the proxy-based strategies have been used in various applications, most of them rarely consider the improvement of system robustness. Nonlinear Disturbance Observer (NDO) based control is a common

This work was supported by the International Science and Technology Cooperation Program of China (No. 2017YFE0128300), the Fundamental Research Funds for the Central Universities (HUST: 2019kfyRCPY014), and the Research Fund of PLA of China (BWS17J024). *(Corresponding author: Jian Huang and Caihua Xiong)*

Y. Cao, J. Huang, D. Wu and M. Zhang are with the Key Laboratory of Image Processing and Intelligent Control, School of Artificial Intelligence and Automation, Huazhong University of Science and Technology, Wuhan 430074, China (e-mail: cao_yu@mail.hust.edu.cn; huang_jan@mail.hust.edu.cn; drwu@hust.edu.cn; dream_poem@hust.edu.cn).

C.-H. Xiong is with the School of Mechanical Science and Engineering and the State Key Laboratory of Digital Manufacturing Equipment and Technology, Huazhong University of Science and Technology, Wuhan 430074, China (e-mail: chxiong@hust.edu.cn).

Z. Li is with the Department of Automation, University of Science and Technology, Hefei 230026, China. (e-mail: zjli@ieee.org).

Y. Hasegawa is with the Department of Micro-Nano Systems Engineering, Nagoya University, Nagoya 464-8603, Japan (email: hasegawa@mein.nagoya-u.ac.jp).

This article has been accepted for publication in a future issue of this journal, but has not been fully edited. Content may change prior to final publication. Citation information: DOI 10.1109/TMECH.2020.2997041, IEEE/ASME Transactions on Mechatronics

method for improving control performance. The basic idea is to estimate the disturbances/uncertainties from measurable variables before a control action is taken. Consequently, the influence of the disturbances/uncertainties can be suppressed, and the system becomes more robust [18]–[20]. Multiple NDO-based control strategies have been proposed to compensate for the influence of disturbances/uncertainties [21]–[25]. However, to our best knowledge, there are very few researches on the proxy-based control strategy integrated with NDO. This may be due to two challenges. First, most of the proxy-based strategies are model-free control approaches, whereas a typical NDO-based controller requires a mathematical model of the control system. Therefore, the integration of proxy-based strategy and NDO is not straightforward. Second, a more rigorous analysis is needed to guarantee the stability of the system, which should not be based on a strong conjecture.

This paper proposes an adaptive proxy-based robust control integrated with nonlinear disturbance observer for the position control of PMAs. Our main contributions are:

1) The proposed adaptive proxy-based robust control extends proxy-based sliding mode control from a model-free strategy to a model-based strategy by defining the motion behaviors of the proxy. Accompanied by a nonlinear disturbance observer, the proposed control method retains the original characteristics of smooth and damped motions and greatly improves the robustness of the algorithm.

2) The proposed controller ensures the global stability of the closed-loop system through two stages, in which the controlled object tracks the proxy, and the proxy tracks the reference trajectory, simultaneously. Furthermore, this paper elaborately studies the case when the proxy is not zero and finds that the non-zero proxy mass is capable of regulating the behaviors of the controlled object.

3) Real-world experiments are conducted based on a physical PMA platform for validating the effectiveness of the proposed controller, and the results present better tracking accuracy and robustness under various reference trajectories.

Note that a study presents an extended proxy-based sliding mode control [26]. Compared with [26], this paper proposes a new theoretical proxy-based method by constructing the motion behaviors of the proxy. Integrating with a NDO, this method can strictly guarantee the global stability of the system while improving the robustness and retaining the original characteristics of smooth and damped motions. Meanwhile, this paper quantitatively analyzes the effect of proxy on control performance. It turns out that as the proxy mass increases, the system's tracking errors will gradually approach a bound associated with estimation errors of the system's uncertainties/disturbances. To the best of our knowledge, this is the first study to investigate the effect of the virtual proxy on the physical plant.

The rest of this paper is organized as follows. Section II introduces the three-element model of the PMA with the lumped disturbances. Section III first proposes the APRC and then extends the APRC to APRC-NDO to improve the system robustness. Section IV presents real-world experiments to demonstrate the effectiveness and robustness of the APRC-NDO. Finally, Section V draws conclusions.

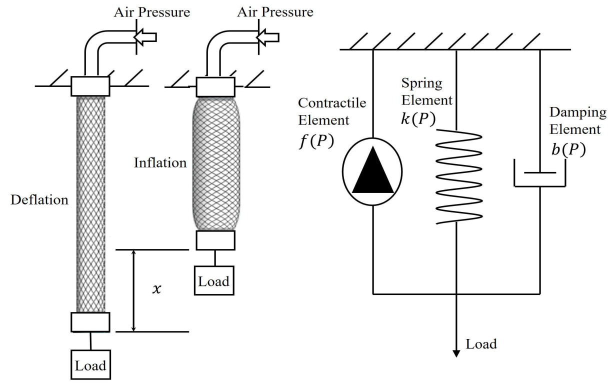

Fig. 1. The PMA and its three-element model.

II. The Three-Element Model of the PMA

The generalized three-element model of the PMA is shown in Fig. 1 [27]. The contractile length varies with the air pressure of inner bladder. The dynamics of the PMA is:

$$\begin{cases} m\ddot{x} + b(P)\dot{x} + k(P)x = f(P) - mg \\ b_i(P) = b_{i0} + b_{i1}P \quad (inflation) \\ b_d(P) = b_{d0} + b_{d1}P \quad (deflation) \\ k(P) = k_0 + k_1 P \\ f(P) = f_0 + f_1 P \end{cases} \tag{1}$$

where m, x, P are the mass of load, the contractile length of PMA, and the air pressure, respectively. $b(P)$, $f(P)$, $k(P)$ are the damping coefficient, the contractile force, and the spring coefficient, respectively.

Let $\tau(t)$ denote the sum of unmodeled uncertainties, including unmodeled dynamics, friction, inaccurate parameters, and changing loads, etc. The dynamics of the PMA can be rewritten as a typical second-order nonlinear model:

$$\begin{cases} \ddot{x} = f(x,\dot{x}) + b(x,\dot{x})u + \tau(t) \\ f(x,\dot{x}) = \frac{1}{m}(f_0 - mg - b_0\dot{x} - k_0 x) \\ b(x,\dot{x}) = \frac{1}{m}(f_1 - b_1\dot{x} - k_1 x) \end{cases} \tag{2}$$

where u is the air pressure, and $f(x,\dot{x})$ and $b(x,\dot{x})$ are nonlinear terms related to the system states.

Lemma 1 [28]: Given a differentiable continuous function $\Psi(t)$, $\forall t \in [t_0, t_1]$ satisfying $\sigma_1 \leq |\Psi(t)| \leq \sigma_2$ with positive constant σ_1 and σ_2. The derivative $\dot{\Psi}(t)$ is also bounded.

Assumption 1 [29]: For the system unknown lumped disturbance $\tau(t)$:$R^+ \rightarrow R$, there exists an unknown positive constant ε such that $\forall t \in R^+$ satisfy $|\tau(t)| < \varepsilon$.

III. Adaptive Proxy-based Robust Control Integrated with Nonlinear Disturbance Observer

A. Adaptive Proxy-based Robust Control

The objective of this study is to drive the trajectory of the PMA to track the desired trajectory. In our proxy-based robust controller, an imaginary object called "proxy", assumed to be

This article has been accepted for publication in a future issue of this journal, but has not been fully edited. Content may change prior to final publication. Citation information: DOI 10.1109/TMECH.2020.2997041, IEEE/ASME Transactions on Mechatronics

connected to the physical actuator, is presented. Before introducing the APRC, we define the following sliding manifolds:

$$S_q = \dot{x}_d - \dot{x} + c_1(x_d - x) + c_2 \int (x_d - x)\, dt \quad (3)$$

$$S_p = \dot{x}_d - \dot{x}_p + c_1(x_d - x_p) + c_2 \int (x_d - x_p)\, dt \quad (4)$$

where c_1 and c_2 are positive constants, x_d the desired trajectory, and x_p and x the proxy position and the PMA's displacement, respectively.

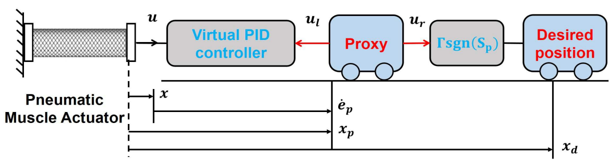

Fig. 2. The principle of proxy-based robust control.

First of all, we design a relationship between the proxy and the controlled object to satisfy:

$$\dot{S}_q + K_p(x_p - x) + K_i \int (x_p - x)\, dt + K_d(\dot{x}_p - \dot{x}) + \tau = 0 \quad (5)$$

where K_p, K_i and K_d are positive constants.

Remark 1. *Traditionally, once the sliding manifold S_q is defined, the controller can be designed using $\dot{S}_q = -k \cdot \mathrm{sgn}(S_q)$, which is known as the sliding mode control and may cause severe chattering. Hence, our idea of introducing the proxy is to replace $-k \cdot \mathrm{sgn}(S_q)$ by a PID controller to establish a connection between the controlled object and the proxy, as shown in Fig. 2. Note that (5) can also be rewritten as:*

$$\dot{\mathbf{X}} = \begin{bmatrix} 0 & 1 & 0 \\ 0 & 0 & 1 \\ 0 & -c_2 & -c_1 \end{bmatrix} \mathbf{X} + \begin{bmatrix} 0 \\ 0 \\ 1 \end{bmatrix} u_l + \begin{bmatrix} 0 \\ 0 \\ 1 \end{bmatrix} \rho \quad (6)$$

where $\rho = \ddot{x}_d + c_1\dot{x}_d + c_2 x_d + \tau$, $\mathbf{X} = [\int x dt, x, \dot{x}]$, and

$$u_l = K_p(x_p - x) + K_i \int (x_p - x)\, dt + K_d(\dot{x}_p - \dot{x}). \quad (7)$$

It is clear that (6) can be regarded as a local relation between the controlled object and the proxy. This is a linear system with PID control, where $\mathbf{X}$ is the system's states, x_p regarded as the desired trajectory, and $\ddot{x}_d$, $\dot{x}_d$ and x_d varying parameters unrelated to the system's states. This PID controller drives the PMA's trajectory x to track the proxy's trajectory x_p, when the controller parameters are properly tuned based on the following stability condition.

Hence, bringing (2) and (3) into (5), the control signal fed into the PMA can be computed:

$$u = \frac{1}{b(x, \dot{x})}[\ddot{x}_d + c_1(\dot{x}_d - \dot{x}) + c_2(x_d - x) - f(x, \dot{x}) + K_p(x_p - x) + K_i \int (x_p - x)\, dt + K_d(\dot{x}_p - \dot{x})]. \quad (8)$$

However, x_p is unknown, and x_p should be driven to approach the desired trajectory x_d to fulfill the tracking tasks. A common idea is to use a sign function to ensure the manifold $S_p \to 0$. Hence, we generate the control signal of proxy u_r between the desired trajectory and the proxy, i.e.,

$$u_r = \hat{\Gamma} \cdot \mathrm{sgn}(S_p) \quad (9)$$

where $\mathrm{sgn}(S_p)$ is the signum function. $\hat{\Gamma}$ is the adaptive gain of the sliding surface S_p, and the corresponding optimal constant of $\hat{\Gamma}$ is Γ^*.

The adaptive law is described as:

$$\dot{\hat{\Gamma}} = \begin{cases} \gamma|S_p|, & |S_p| \geq \delta \\ 0, & |S_p| < \delta \end{cases}, \hat{\Gamma}(0) = 0 \quad (10)$$

where γ is a positive constant that regulates the adaptive rate. δ is a boundary layer. When the system achieves a steady-state, $|S_p|$ is small enough, so that $\hat{\Gamma}$ will reach an upper bound instead of monotonically increasing.

Remarkably, the proxy is affected by u_r and u_l, simultaneously, as shown in Fig. 2, and they are not force signals in the traditional sense. Hence, we cannot directly use Newton's law to establish the relationship between the motion behaviors of the proxy and u_r, u_l. Besides, it is necessary to define such property to ensure the realization of tracking and the system's stability. Similar to Newton's law, we define the behavior of the proxy under the effects of u_r and u_l. Let $m_p > 0$ be the so-called proxy mass. Then,

$$m_p \dot{S}_p = -u_r + u_l. \quad (11)$$

The effect of $-u_r + u_l$ is similar to the resultant force on the proxy while $m_p \dot{S}_p$ can be seen as the motion principle of the proxy. Note that this property can be arbitrarily defined according to the specific situation, as long as the stability of the closed-loop system can be ensured.

Combining (4), (7), (9), and (11), the trajectory of the proxy is presented as:

$$\ddot{x}_p = \frac{1}{m_p}[\hat{\Gamma}\mathrm{sgn}(S_p) - K_p(x_p - x) - K_i \int (x_p - x)\, dt - K_d(\dot{x}_p - \dot{x})] + \ddot{x}_d + c_1(\dot{x}_d - \dot{x}_p) + c_2(x_d - x_p). \quad (12)$$

Once x_p is determined, the control signal of the PMA can then be computed from (4), (8) and (12).

For the convenience of presentation, we first define $\mathbf{K}_m = diag\{K_i c_2, \varpi, K_d\}$ with $\varpi = K_p c_1 - K_i - K_d c_2$.

Theorem 1. *The norm of tracking error between the proxy states $\mathbf{X}_p = [\int x_p dt, x_p, \dot{x}_p]^T$ and the system states $\mathbf{X} = [\int x dt, x, \dot{x}]^T$ is uniformly ultimately bounded, and a sliding motion on the surface (4) can be guaranteed when the APRC satisfies:*

$$m_p > 0, \lambda(\mathbf{K}_c) > 0, \Gamma^* \geq \lambda_2(K_p + K_i + K_d), \varpi > 0$$

where $\lambda(\cdot)$ and $\lambda_{\min}(\cdot)$ denote the eigenvalues and the minimum eigenvalue of the matrix, respectively.

$$\lambda_2 = \frac{(c_1 + c_2 + 1)\varepsilon}{\lambda_{\min}(\mathbf{K}_m)}, \mathbf{K}_c = \begin{bmatrix} K_p c_2 + K_i c_1 & K_i + K_d c_2 \\ K_i + K_d c_2 & K_p + K_d c_1 \end{bmatrix}.$$

Proof: Due to $\lambda(\mathbf{K}_c) > 0$, a Lyapunov candidate is defined as $V = V_1 + V_2 + V_3 > 0$ with

$$V_1 = \frac{1}{2}m_p S_p^2 + \frac{1}{2}S_q^2 \quad (13)$$

$$\begin{aligned} V_2 &= \frac{1}{2}\begin{bmatrix} e_p & \dot{e}_p \end{bmatrix}\mathbf{K}_c\begin{bmatrix} e_p \\ \dot{e}_p \end{bmatrix} \\ &= \frac{1}{2}(K_p + K_d c_1 - K_i - K_d c_2)\dot{e}_p^2 \\ &\quad + \frac{1}{2}(K_p c_2 + K_i c_1 - K_i - K_d c_2)e_p^2 \\ &\quad + \frac{1}{2}(K_i + K_d c_2)(e_p + \dot{e}_p)^2 \end{aligned} \tag{14}$$

$$V_3 = \frac{1}{2\gamma}\tilde{\Gamma}^2 \tag{15}$$

where $e_p = \int (x_p - x)\, dt$ and $\tilde{\Gamma}=\hat{\Gamma} - \Gamma^*$.

From (7)-(11), it follows that

$$m_p \dot{S}_p = -\hat{\Gamma}\mathrm{sgn}(S_p) + K_p \dot{e}_p + K_i e_p + K_d \ddot{e}_p. \tag{16}$$

According to (3)-(5), we have

$$\dot{S}_q = -K_p \dot{e}_p - K_i e_p - K_d \ddot{e}_p - \tau \tag{17}$$

$$S_p = S_q - (\ddot{e}_p + c_1 \dot{e}_p + c_2 e_p). \tag{18}$$

Integrating (10)-(18), the derivatives of V_1, V_2 and V_3 are:

$$\begin{aligned} \dot{V}_1 &= S_p(-\hat{\Gamma}\mathrm{sgn}(S_p) + K_p \dot{e}_p + K_i e_p + K_d \ddot{e}_p) \\ &\quad + S_q(-K_p \dot{e}_p - K_i e_p - K_d \ddot{e}_p - \tau) \\ &= -\hat{\Gamma}|S_p| - \tau S_q + (K_p \dot{e}_p + K_i e_p + K_d \ddot{e}_p)(S_p - S_q) \\ &= -\hat{\Gamma}|S_p| - \tau S_q - K_d \ddot{e}_p^2 - K_p c_1 \dot{e}_p^2 - K_i c_2 e_p^2 \\ &\quad - (K_p + K_d c_1)\dot{e}_p \ddot{e}_p - (K_i + K_d c_2) e_p \ddot{e}_p \\ &\quad - (K_p c_2 + K_i c_1) e_p \dot{e}_p \end{aligned} \tag{19}$$

$$\begin{aligned} \dot{V}_2 &= (K_p + K_d c_1)\dot{e}_p \ddot{e}_p + (K_p c_2 + K_i c_1) e_p \dot{e}_p \\ &\quad + (K_i + K_d c_2)\dot{e}_p^2 + (K_i + K_d c_2) e_p \ddot{e}_p. \end{aligned} \tag{20}$$

$$\dot{V}_3 = \frac{1}{\gamma}\tilde{\Gamma}\dot{\tilde{\Gamma}} = \tilde{\Gamma}\,|S_p| = \hat{\Gamma}\,|S_p| - \Gamma^*\,|S_p|\,. \tag{21}$$

Then, it follows that

$$\dot{V}_1 + \dot{V}_2 = -\hat{\Gamma}|S_p| - \tau S_q - K_d \ddot{e}_p^2 - \varpi \dot{e}_p^2 - K_i c_2 e_p^2. \tag{22}$$

Note that

$$\Gamma^* \geq \frac{(K_p + K_i + K_d)(1 + c_1 + c_2)}{\min(K_i c_2, \varpi, K_d)}\varepsilon \geq \varepsilon. \tag{23}$$

From (17)-(23), we have

$$\begin{aligned} \dot{V} &= \dot{V}_1 + \dot{V}_2 + \dot{V}_3 \\ &= -\Gamma^*\,|S_p| - \tau S_q - K_d \ddot{e}_p^2 - \varpi \dot{e}_p^2 - K_i c_2 e_p^2 \\ &\leq -\varepsilon\,|S_q| + \varepsilon\,|\ddot{e}_p + c_1 \dot{e}_p + c_2 e_p| \\ &\quad - \tau S_q - K_d \ddot{e}_p^2 - \varpi \dot{e}_p^2 - K_i c_2 e_p^2 \\ &\leq \varepsilon(1 + c_1 + c_2)\,\|\mathbf{e}_p\| - \lambda_{\min}(\mathbf{K}_m)\|\mathbf{e}_p\|^2 \\ &= -\,\|\mathbf{e}_p\|\,[\lambda_{\min}(\mathbf{K}_m)\,\|\mathbf{e}_p\| - \varepsilon(1 + c_1 + c_2)] \end{aligned} \tag{24}$$

where $\mathbf{e}_p = \mathbf{X}_p - \mathbf{X} = \begin{bmatrix} e_p & \dot{e}_p & \ddot{e}_p \end{bmatrix}^T$. It is easy to see that after a sufficiently long time

$$\|\mathbf{e}_p\| \leq \lambda_2. \tag{25}$$

As a result, $\|\mathbf{e}_p\|$ is uniformly ultimately bounded.

Define a new Lyapunov candidate as:

$$V_p = \frac{1}{2}m_p S_p^2 + \frac{1}{2\gamma}\tilde{\Gamma}^2. \tag{26}$$

It follows from (16) that

$$\begin{aligned} \dot{V}_p &= m_p S_p \dot{S}_p + \frac{1}{\gamma}\tilde{\Gamma}\dot{\tilde{\Gamma}} \\ &= -\Gamma^*\,|S_p| + (K_p \dot{e}_p + K_i e_p + K_d \ddot{e}_p) S_p \\ &\leq -\Gamma^*\,|S_p| + \lambda_2(K_p + K_i + K_d) S_p \\ &\leq 0. \end{aligned} \tag{27}$$

When $||\mathbf{e}_p||$ is uniformly ultimately bounded, the achievement of a sliding motion on the surface (4) is guaranteed.

This completes the proof. ■

Remark 2. *The stability analysis of the system has two motion phases. First, the norm of the tracking error between the proxy states $\mathbf{X}_p$ and the system states $\mathbf{X}$ is uniformly ultimately bounded. This indicates that the system states converge to the proxy states. Then, the achievement of sliding motion on the surface (4) means that the proxy tracks the reference trajectory, theoretically. In summary, the system states are capable of indirectly tracking the reference, and the stability of the closed-loop system is guaranteed.*

Corollary 1. *If inequality (25) holds, and initially $x_p = x_d$, then, as the proxy mass m_p increases, S_q will gradually approach a bound associated with the upper bound of the lumped disturbances.*

$$\lim_{m_p \to \infty} |S_q| \leq \lambda_2(c_1 + c_2 + 1). \tag{28}$$

Proof: From (16), it follows that

$$|\dot{S}_p| = \frac{1}{m_p}| - \Gamma^*\mathrm{sgn}(S_p) + K_p \dot{e}_p + K_i e_p + K_d \ddot{e}_p|. \tag{29}$$

Since the system is globally uniformly ultimately bounded and a limited Γ^*, we have

$$\lim_{m_p \to \infty} |\dot{S}_p| = 0. \tag{30}$$

The proxy mass m_p is a fixed value in each experiment. Let t_f be the finite duration of the experiment. Then,

$$S_p = \int_0^{t_f} \dot{S}_p dt + \upsilon \tag{31}$$

where υ is the initial value of $x_d - x_p$, which equals zero. Hence, it follows that

$$|S_p| = |\int_0^{t_f} \dot{S}_p dt| \leq \int_0^{t_f} |\dot{S}_p| dt. \tag{32}$$

Combining (30) and (32), we can obtain

$$\lim_{m_p \to \infty} |S_p| = 0. \tag{33}$$

Considering (18) and (25), after a sufficiently long time

$$\begin{aligned} |S_q| &\leq |S_p| + |\ddot{e}_p + c_1 \dot{e}_p + c_2 \ddot{e}_p| \\ &\leq |S_p| + \lambda_2(c_1 + c_2 + 1). \end{aligned} \tag{34}$$

Finally,

$$\lim_{m_p \to \infty} |S_q| \leq \lambda_2(c_1 + c_2 + 1). \tag{35}$$

According to the above results, when the proxy mass m_p approaches positive infinity, S_q will approach a bound associated with the the upper bound of the lumped disturbances. This means that m_p can be used to regulate the behaviors of the PMA. Normally, it should be sufficiently large, so that the proxy trajectory will track the reference accurately and realize a damped response.

This completes the proof. ∎

B. Adaptive Proxy-based Robust Control Integrated with Nonlinear Disturbance Observer

The previous analysis indicates that the APRC can suppress system uncertainties and ensure the uniformly ultimate boundedness of the system states. However, unlike fast-response motors, the response of the PMA system tends to be relatively slow. The excessive gain Γ^* leads to control accuracy degradation and system instability. Therefore, a nonlinear disturbance observer is considered to handle the system uncertainties and increase the system robustness. According to Lemma 1 and Assumption 1, we have

$$|\dot{\tau}| \leq \mu \tag{36}$$

where μ being an unknown constant.

We define an auxiliary variable z to design the nonlinear disturbance observer, as shown

$$\left\{ \begin{array}{c} \hat{\tau} = z + \kappa \dot{x} \\ \dot{z} = -\kappa(f(x,\dot{x}) + b(x,\dot{x})u + \hat{\tau}) \end{array} \right. \tag{37}$$

where $\hat{\tau}$ is the estimation of disturbances and κ is a constant gain. Therefore, the derivative of $\hat{\tau}$ is

$$\dot{\hat{\tau}} = \dot{z} + \kappa \ddot{x} = \kappa \tilde{\tau} \tag{38}$$

where $\tilde{\tau} = \tau - \hat{\tau}$. Subtracting both sides of (38) from $\dot{\tau}$, we have $\dot{\tilde{\tau}} = \dot{\tau} - \kappa\tilde{\tau}$ with $\dot{\tilde{\tau}} = \dot{\tau} - \dot{\hat{\tau}}$.

Defining a Lyapunov function

$$V_\tau(\tilde{\tau}) = \frac{1}{2}\tilde{\tau}^2 \tag{39}$$

and evaluating $\dot{V}_\tau(\tilde{\tau})$ along (39)

$$\begin{aligned} \dot{V}_\tau(\tilde{\tau}) &= \tilde{\tau}\dot{\tilde{\tau}} = \tilde{\tau}(\dot{\tau} - \kappa\tilde{\tau}) \\ &\leq \mu\,|\tilde{\tau}| - \kappa\tilde{\tau}^2 \\ &= -\,|\tilde{\tau}|\,(\kappa\,|\tilde{\tau}| - \mu). \end{aligned} \tag{40}$$

Therefore, the estimation error is bounded by

$$|\tilde{\tau}| \leq \tilde{\varepsilon} \tag{41}$$

where $\tilde{\varepsilon} = \mu/\kappa$.

To integrate the nonlinear disturbance observer into the APRC, we only need to redefine (5) as:

$$\begin{aligned} \dot{S}_q + K_p(x_p - x) + K_i \int (x_p - x)\,dt \\ + K_d(\dot{x}_p - \dot{x}) + \tilde{\tau} = 0. \end{aligned} \tag{42}$$

Similarly, bringing (2) and (3) into (42), the control signal of the PMA system is:

$$\begin{aligned} u = \frac{1}{b(x,\dot{x})}[\ddot{x}_d + c_1(\dot{x}_d - \dot{x}) + c_2(x_d - x) - f(x,\dot{x}) \\ + K_p(x_p - x) + K_i \int (x_p - x)\,dt + K_d(\dot{x}_p - \dot{x}) - \hat{\tau}]. \end{aligned} \tag{43}$$

Theorem 2. *The norm of $\tilde{\mathbf{e}}_p = [e_p, \dot{e}_p, \ddot{e}_p, \tilde{\tau}]^T$ is uniformly ultimately bounded, and a sliding motion on the surface (4) can be guaranteed when the APRC-NDO satisfies:*

$$m_p > 0, \lambda(\mathbf{K}_c) > 0, \Gamma^* \geq \lambda_2'(K_p + K_i + K_d), \varpi > 0$$

where $\mathbf{K}_m' = diag\{K_i c_2, \varpi, K_d, \kappa\}$, and

$$\lambda_2' = \frac{\tilde{\varepsilon}(1 + c_1 + c_2) + \mu}{\lambda_{\min}(\mathbf{K}_m')}$$

Proof: We define a new Lyapunov candidate

$$V' = V_1 + V_2 + V_3 + \frac{1}{2}\tilde{\tau}^2 \tag{44}$$

and note that $\Gamma^* \geq \lambda_2'(K_p + K_i + K_d) \geq \tilde{\varepsilon}$.

From (16), (21), (36)-(39) and (42), the derivative of V' is:

$$\begin{aligned} \dot{V}' &= -\Gamma^*\,|S_p| - \tilde{\tau}S_q - K_d\ddot{e}_p^2 - \varpi\dot{e}_p^2 - K_i c_2 e_p^2 + \tilde{\tau}\dot{\tilde{\tau}} \\ &\leq -\tilde{\varepsilon}\,|S_q| + \tilde{\varepsilon}\,|\ddot{e}_p + c_1\dot{e}_p + c_2 e_p| - \tilde{\tau}S_q \\ &\quad - K_d\ddot{e}_p^2 - \varpi\dot{e}_p^2 - K_i c_2 e_p^2 + \mu\,|\tilde{\tau}| - \kappa\tilde{\tau}^2 \\ &\leq [\tilde{\varepsilon}(1 + c_1 + c_2) + \mu]\,\|\tilde{\mathbf{e}}_p\| - \lambda_{\min}(\mathbf{K}_m')\|\tilde{\mathbf{e}}_p\|^2 \\ &= -\,\|\tilde{\mathbf{e}}_p\|\,(\lambda_{\min}(\mathbf{K}_m')\,\|\tilde{\mathbf{e}}_p\| - [\tilde{\varepsilon}(1 + c_1 + c_2) + \mu]) \end{aligned} \tag{45}$$

Thus, $\tilde{\mathbf{e}}_p$ is uniformly ultimately bounded by

$$\|\tilde{\mathbf{e}}_p\| \leq \lambda_2' \tag{46}$$

In this situation, by applying the similar technique in (27), the achievement of a sliding motion on (4) is guaranteed.

$$V_p' = \frac{1}{2}m_p S_p^2 + \frac{1}{2\gamma}\tilde{\Gamma}^2. \tag{47}$$

Thus, the derivative of V_p' is expressed as:

$$\begin{aligned} \dot{V}_p' &= m_p S_p \dot{S}_p + \tilde{\Gamma}\dot{\tilde{\Gamma}} \\ &\leq -\Gamma^*\,|S_p| + \lambda_2'(K_p + K_i + K_d)S_p \\ &\leq 0 \end{aligned} \tag{48}$$

This completes the proof. ∎

Corollary 2. *If inequality (46) holds, and initially $x_p = x_d$, then, as the proxy mass m_p increases, S_q will gradually approach a bound associated with estimation errors of the lumped disturbances.*

$$\lim_{m_p \to \infty} |S_q| \leq \lambda_2'(c_1 + c_2 + 1). \tag{49}$$

Proof: This corollary can be easily proven by using the similar method given in the Proof of Corollary 1. ∎

IV. Experiments

A. Experiment Setup

In the physical system, the board (NI-PCI 6052E) enabled A/D and D/A to collect the sensory data and transmitted the control signal to an electromagnetic proportional valve for regulating the inner pressure of the PMA. The air compressor provided compressed air and was connected to the PMA through the electromagnetic proportional valve. Consequently, the displacement of the PMA can be controlled by feedbacking the displacement, as shown in Fig. 3. The PMA was Festo

DMSP-20-200N-RM-RM fluidic muscle with an internal diameter of 20 mm, nominal length of 200 mm, and an operating pressure range from 0 to 6 bar. The Festo VPPM-6L-L-1-G18-0L10H-V1P proportional valve was used to regulate the pressure inside the PMA. The displacement sensor was GA-75 whose measurement range was 0-150 mm.

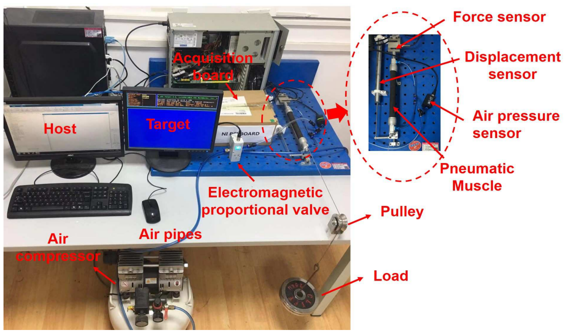

Fig. 3. The PMA system.

The proposed method does not require an accurate three-element model of the PMA. So, we used the identified parameters of a similar PMA in [11] (see Table I).

We designed two reference trajectories. The first was a fixed frequency sinusoid:

$$x_d = A_x \sin(2\pi f_x t) + B_x \tag{50}$$

where $A_x = 0.015$ m, $f_x = 0.25$ Hz, and $B_x = 0.015$ m. The second was a sine wave whose frequency changed linearly from 0.1 Hz to 0.5 Hz within 20 s. The sampling time was set to 0.001 s.

TABLE I
THE MODEL PARAMETERS.

Parameter	Value (Unit)	Parameter	Value (Unit)
f_0	-202.32 (N)	f_1	0.00721 (N/Pa)
k_{01}	18063.0 (N/m)	k_{02}	0.01051 (N/(m.Pa))
k_{11}	-0.2132 (N/m)	k_{12}	90638.0 (N/(m.Pa))
b_{0i}	6435.31 (N.s/m)	b_{1i}	0.10023 (N.s/(m.Pa))
b_{0d}	2522.01 (N.s/m)	b_{1d}	0.00321 (N.s/(m.Pa))

The maximum absolute error (MAE), the integral of absolute error (IAE) and the relative tracking accuracy (RTE) were used as our performance measurements:

$$MAER^a = Max(|x_d(t) - x(t)|_{t=1}^{N}) \tag{51}$$

$$IAER^b = \frac{1}{N}\sum_{t=1}^{N} |x_d(t) - x(t)| \tag{52}$$

$$RTER^c = \frac{(\sum\limits_{t=1}^{N} |x_d(t) - x(t)|)/N}{x_a} \times 100\% \tag{53}$$

where N is the total sampling time. x_a is the maximum running displacement of the PMA.

The following set of control parameters of the APRC-NDO was used in all experiments: $c_1 = 177.4$, $c_2 = 174.4$, $K_p = 2473.5$, $K_i = 1916$, $K_d = 194.2$, $\kappa = 15952$, $\gamma = 10$. Note that the parameter selections of all the control strategies were based on an optimization algorithm, called switch-mode firefly algorithm (SMFA). More related details can be found in [30].

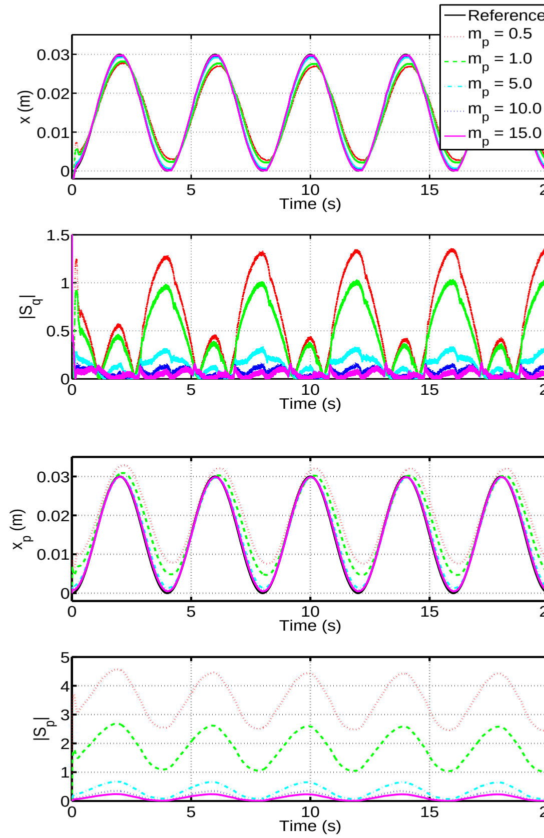

Fig. 4. Tracking performance of the APRC-NDO with different m_p values.

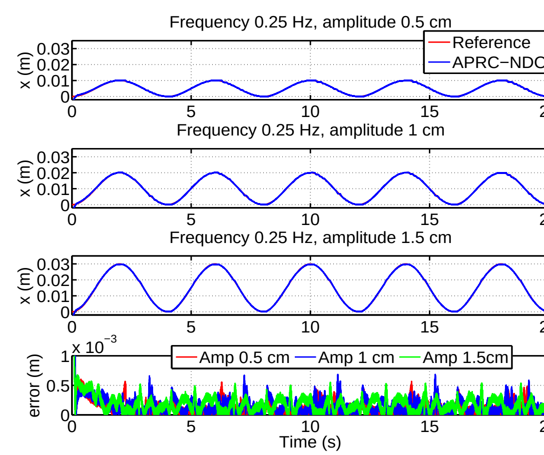

Fig. 5. Tracking performance of the APRC-NDO with different amplitudes of the desired trajectories.

B. Experimental Results

Fig. 4 showed the experimental results that verified the Corollary 1. In this experiment, we selected a fixed Γ^* to demonstrate the influence of $m_p = \{0.5, 1.0, 5.0, 10.0, 15.0\}$. As m_p increased, the tracking accuracy improved, and the variation of S_q significantly decreased. Meanwhile, x_p tracked the reference trajectory more accurately and $|S_p| \to 0$.

Then, we intended to verify the experimental results of the proposed control strategy with different amplitudes of the desired trajectories, as shown in Fig. 5. The corresponding

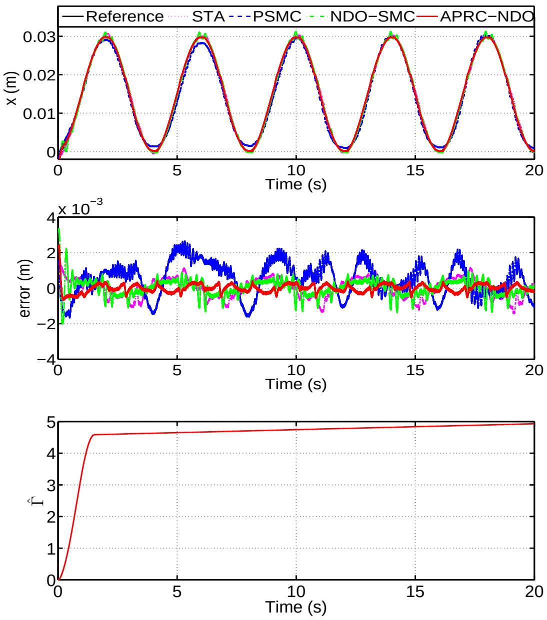

Fig. 6. Tracking performance of different control strategies with the fixed-frequency sinusoidal reference (0.25 Hz).

TABLE II
TRACKING PERFORMANCE OF DIFFERENT CONTROL STRATEGIES WITH THE FIXED-FREQUENCY SINUSOIDAL REFERENCE (0.25 Hz).

	MAE	IAE	RTE
APRC-NDO	5.5×10^{-4} (m)	1.6×10^{-4} (m)	0.5%
PSMC	2.7×10^{-3} (m)	8.9×10^{-4} (m)	2.9%
NDO-SMC	1.4×10^{-3} (m)	3.5×10^{-4} (m)	1.2%
STA	1.5×10^{-3} (m)	4.5×10^{-4} (m)	1.5%
PID [8]	4.0×10^{-3} (m)	1.5×10^{-3} (m)	6.0%

control performances were similar, and the control parameters did not change for this experiment, which indicated that the proposed method is applicable to various applications.

Next, for a fair comparison, the control parameters for all the strategies {APRC-NDO, NDO-SMC, super twisting algorithm (STA), PSMC} were adjusted with the fixed-frequency sinusoidal reference ($f_x = 0.25$ Hz, $A_x = 0.015$ m, $B_x = 0.015$ m) by the SMFA. Fig. 6 showed the corresponding performance of different control strategies, and the corresponding MAEs, IAEs and RTEs of all five control strategies were shown in Table II. We replaced the *sign* function of the NDO-SMC with a *sat* function to eliminate chattering. In spite of the inaccurate model parameters in Table I, the NDO-SMC and STA were capable of handling the uncertainties and achieving favorable performance. Meanwhile, the basic PSMC enabled the PMA to track the reference with acceptable precision, since it is a model-free strategy, not affected by inaccurate model parameters. However, its performance was still unsatisfied than APRC-NDO. Besides, according to our previous study [8], although the traditional PID controller tracked the reference trajectory, the performance was worse than the proposed strategy. On the other hand, because we had $|S_p| \rightarrow 0$, the adaptive coefficient $\hat{\Gamma}$ gradually tended to be a fixed value, instead of monotonically increasing.

Based on the previous tuned control parameters, Fig. 7 showed the tracking performance of different control strategies with the varying-frequency (0.1-0.5Hz) sinusoidal reference. Although the NDO-SMC behaved well in the steady-state, it had a large oscillation at the beginning. On the contrary, the STA performed well at the beginning, but it could not effectively track the reference as the frequency increased. Still, the PSMC tracked the reference with acceptable precision. The proposed APRC-NDO performed the best among all four control strategies, although it had a relatively little oscillation at the beginning. This was because the APRC-NDO needed some time to drive the states of the PMA into the boundary [see (25) and (46)]. After that, the proposed APRC-NDO could handle the system disturbances/uncertainties and achieve accurate tracking. Actually, the NDO is very important, because the uncertainties/disturbances of the system relate to the frequency of PMA's trajectory, and the varying frequency causes the growth of the system's uncertainties/disturbances. The SMC and APRC integrated with NDO can better handle the uncertainties/disturbances of the system.

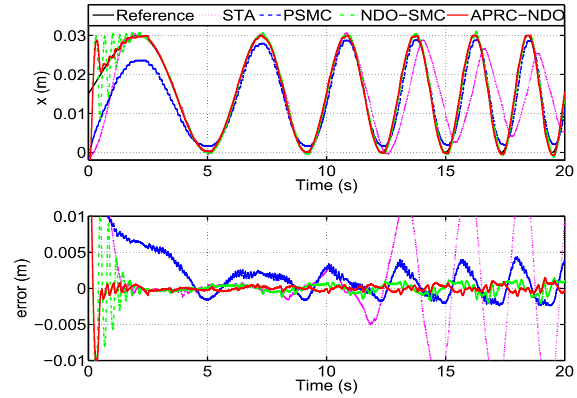

Fig. 7. Tracking performance of different control strategies with the varying-frequency sinusoidal reference ($0.1 - 0.5$ Hz).

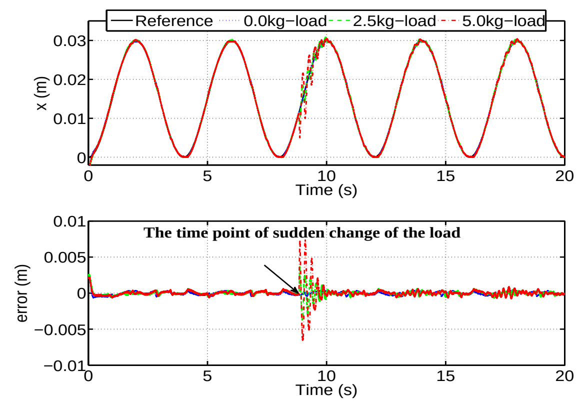

Fig. 8. Tracking performance of the APRC-NDO with a sudden change of load.

To further investigate the robustness of the proposed control strategy, we first designed an experiment, in which a sudden change of the load (2.5kg-load or 5.0kg-load) was added to the PMA during operation, as shown in Fig. 8. It is seen that the trajectory of the PMA deviated significantly from

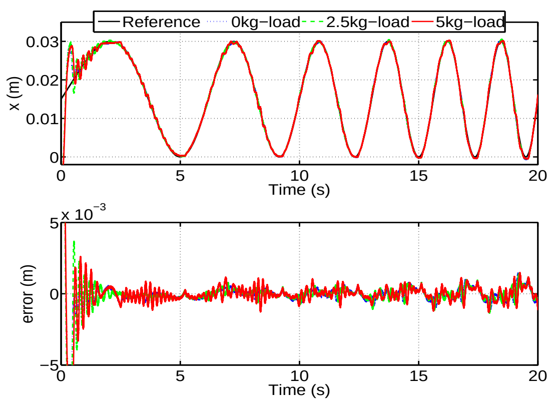

Fig. 9. Tracking performance of the APRC-NDO with the PMA attaching different loads.

the reference, and the greater the sudden disturbance, the further it deviated. Moreover, additional experiments were conducted for tracking the varying-frequency (0.1-0.5 Hz) reference with different loads, as shown in Fig. 9. Generally, they were very robust to the changing loads. However, the fixed parameters of the NDO can only handle a certain amount of disturbances. When the disturbance is beyond a certain degree, the parameters of NDO have to be re-tuned.

V. Conclusion

This paper presented a robust control strategy, APRC-NDO, for the PMA. The APRC-NDO can realize a damped response and regulate the behaviors of the PMA via a virtual proxy, as well as handle the system uncertainties/disturbances to improve the robustness. The tracking states of the PMA were proven to be uniformly ultimately bounded through two motion phases. Finally, extensive experiments demonstrated the superior performance of the APRC-NDO.

References

[1] M.A.M. Dzahir and S.-i. Yamamoto, "Recent Trends in Lower-Limb Robotic Rehabilitation Orthosis: Control Scheme and Strategy for Pneumatic Muscle Actuated Gait Trainers,", *Robotics*, vol. 3, no. 2, pp. 120-148, Mar. 2014.

[2] J. Cao, S. Q. Xie and R. Das, "MIMO Sliding Mode Controller for Gait Exoskeleton Driven by Pneumatic Muscles," *IEEE Trans. Control Syst. Technol.*, vol. 26, no. 1, pp. 274-281, Jan. 2018.

[3] Z. Li, B. Huang, A. Ajoudani, C. Yang, C. Su and A. Bicchi, "Asymmetric Bimanual Control of Dual-Arm Exoskeletons for Human-Cooperative Manipulations," *IEEE Trans. Robot.*, vol. 34, no. 1, pp. 264-271, Feb. 2018.

[4] Z. Li, B. Huang, Z. Ye, M. Deng and C. Yang, "Physical Human-Robot Interaction of a Robotic Exoskeleton By Admittance Control," *IEEE Trans. Ind. Electron.*, vol. 65, no. 12, pp. 9614-9624, Dec. 2018.

[5] D. G. Caldwell, G. A. Medrano-Cerda and M. Goodwin, "Control of Pneumatic Muscle Actuators," *IEEE Control Syst.*, vol. 15, no. 1, pp. 40-48, Feb. 1995.

[6] G. Andrikopoulos, G. Nikolakopoulos and S. Manesis, "Advanced Nonlinear PID-Based Antagonistic Control for Pneumatic Muscle Actuators," *IEEE Trans. Ind. Electron.*, vol. 61, no. 12, pp. 6926-6937, Dec. 2014.

[7] J. Huang, J. Qian, L. Liu, Y. Wang, C. Xiong, S. Ri, "Echo State Network based Predictive Control with Particle Swarm Optimization for Pneumatic Muscle Actuator," *J. Frankl. Inst.*, vol. 353, no. 12, pp. 2761-2782, 2016.

[8] J. Huang, Y. Cao, C. Xiong and H. Zhang, "An Echo State Gaussian Process-Based Nonlinear Model Predictive Control for Pneumatic Muscle Actuators," *IEEE Trans. Autom. Sci. Eng.*, vol. 16, no. 3, pp. 1071-1084, July 2019.

[9] J. H. Lilly and L. Yang, "Sliding Mode Tracking for Pneumatic Muscle Actuators in Opposing Pair Configuration," *IEEE Trans. Control Syst. Technol.*, vol. 13, no. 4, pp. 550-558, July 2005.

[10] S.Q. Xie, P.K. Jamwal, "An Iterative Fuzzy Controller for Pneumatic Muscle Driven Rehabilitation Robot," *Expert Syst. Appl.*, vol. 38, no. 7, pp. 8128-8137, Jul. 2011.

[11] L. Zhu, X. Shi, Z. Chen, H. Zhang and C. Xiong, "Adaptive Servomechanism of Pneumatic Muscle Actuators With Uncertainties," *IEEE Trans. Ind. Electron.*, vol. 64, no. 4, pp. 3329-3337, Apr. 2017.

[12] J. Wu, J. Huang, Y. Wang and K. Xing, "Nonlinear Disturbance Observer-Based Dynamic Surface Control for Trajectory Tracking of Pneumatic Muscle System," *IEEE Trans. Control Syst. Technol.*, vol. 22, no. 2, pp. 440-455, Mar. 2014.

[13] X. Li, Y. Pan, G. Chen and H. Yu, "Adaptive Human-Robot Interaction Control for Robots Driven by Series Elastic Actuators," *IEEE Trans. Robot.*, vol. 33, no. 1, pp. 169-182, Feb. 2017.

[14] R. Kikuuwe, S. Yasukouchi, H. Fujimoto and M. Yamamoto, "Proxy-Based Sliding Mode Control: A Safer Extension of PID Position Control," *IEEE Trans. Robot.*, vol. 26, no. 4, pp. 670-683, Aug. 2010.

[15] M. V. Damme, B. Vanderborght, B. Verrelst, R. V. Ham, F. Daerden, and D. Lefeber, "Proxy-based Sliding Mode Control of a Planar Pneumatic Manipulator, *Int. J. Robotics Res.*, vol. 28, no. 2, pp. 266-284, 2009.

[16] G. Gu, L. Zhu, C. Su, H. Ding and S. Fatikow, "Proxy-Based Sliding-Mode Tracking Control of Piezoelectric-Actuated Nanopositioning Stages," *IEEE/ASME Trans. Mechatron.*, vol. 20, no. 4, pp. 1956-1965, Aug. 2015.

[17] K. Kong, "Proxy-based Impedance Control of a Cable-driven Assistive System," *Mechatronics*, vol. 23, no. 1, pp. 147-153, Feb. 2013.

[18] Y. Yan, J. Yang, Z. Sun, C. Zhang, S. Li and H. Yu, "Robust Speed Regulation for PMSM Servo System With Multiple Sources of Disturbances via an Augmented Disturbance Observer," *IEEE/ASME Trans. Mechatron.*, vol. 23, no. 2, pp. 769-780, Apr. 2018.

[19] J. Han, "From PID to Active Disturbance Rejection Control," *IEEE Trans. Ind. Electron.*, vol. 56, no. 3, pp. 900-906, Mar. 2009.

[20] D. X. Ba, T. Q. Dinh, J. Bae and K. K. Ahn, "An Effective Disturbance-Observer-Based Nonlinear Controller for a Pump-Controlled Hydraulic System," *IEEE/ASME Trans. Mechatron.*, vol. 25, no. 1, pp. 32-43, Feb. 2020.

[21] J. Huang, S. Ri, T. Fukuda and Y. Wang, "A Disturbance Observer based Sliding Mode Control for a Class of Underactuated Robotic System With Mismatched Uncertainties," *IEEE Trans. Autom. Control*, vol. 64, no. 6, pp. 2480-2487, June 2019.

[22] J. Huang, M. Zhang, S. Ri, C. Xiong, Z. Li and Y. Kang, "High-Order Disturbance-Observer-Based Sliding Mode Control for Mobile Wheeled Inverted Pendulum Systems," *IEEE Trans. Ind. Electron.*, vol. 67, no. 3, pp. 2030-2041, Mar. 2020.

[23] Z. Li, J. Li, S. Zhao, Y. Yuan, Y. Kang and C. L. P. Chen, "Adaptive Neural Control of a Kinematically Redundant Exoskeleton Robot Using Brain-Machine Interfaces," *IEEE Trans. Neural Netw. Learn. Syst.*, vol. 30, no. 12, pp. 3558-3571, Dec. 2019.

[24] W. He, Z. Yan, C. Sun and Y. Chen, "Adaptive Neural Network Control of a Flapping Wing Micro Aerial Vehicle With Disturbance Observer," *IEEE Trans. Cybern.*, vol. 47, no. 10, pp. 3452-3465, Oct. 2017.

[25] M. Chen, S. Y. Shao and B. Jiang, "Adaptive Neural Control of Uncertain Nonlinear Systems Using Disturbance Observer," *IEEE Trans. Cybern.*, vol. 47, no. 10, pp. 3110-3123, Oct. 2017.

[26] W. Zhao, A. Song, Y. Cao, "An Extended Proxy-Based Sliding Mode Control of Pneumatic Muscle Actuators," *Appl. Sci.*, vol. 9, no. 8, pp. 1571, 2019.

[27] D. B. Reynolds, D. W. Repperger, C. A. Phillips, and G. Bandry, "Modeling the Dynamic Characteristics of Pneumatic Muscle," *Ann. Biomed. Eng.*, vol. 31, pp. 310-317, Mar. 2003.

[28] L. Zhang, Z. Li and C. Yang, "Adaptive Neural Network Based Variable Stiffness Control of Uncertain Robotic Systems Using Disturbance Observer," *IEEE Trans. Ind. Electron.*, vol. 64, no. 3, pp. 2236-2245, Mar. 2017.

[29] T. P. Zhang and S. S. Ge, "Adaptive Dynamic Surface Control of Nonlinear Systems with Unknown Dead Zone in Pure Feedback Form," *Automatica*, vol. 44, no. 7, pp. 1895-1903, Jul. 2008.

[30] Y. Cao, J. Huang, Z. Huang, X. Tu, and S. Mohammed, "Optimizing Control of Passive Gait Training Exoskeleton Driven by Pneumatic Muscles Using Switch-mode Firefly Algorithm," *Robotica*, vol. 37, no. 12, pp. 2087-2103, Dec. 2019.